Available online at www.sciencedirect.com
SCIENCE DIRECT®
Journal of Power Sources 129 (2004) 188–192
JOURNAL OF POWER SOURCES
www.elsevier.com/locate/jpowsour

Reactivity of lanthanide ferrite SOFC cathodes with YSZ electrolyte

Michael D. Anderson, Jeffry W. Stevenson, Steven P. Simner*

Materials Science Division (MS: K2-44), Pacific Northwest National Laboratory, Department MSIN K2-44, P.O. Box 999, 902 Battelle Boulevard, Richland, WA 99352, USA

Received 9 October 2003; accepted 10 November 2003

Abstract

The reactivity of yttria-stabilized zirconia (YSZ) with compounds of the form $Ln_{0.8}Sr_{0.2}FeO_3$ (Ln = Sm, Pr, Nd and a mixed lanthanide precursor) and $La_{0.8}M_{0.2}FeO_3$ (M = Ba, Ca) was investigated, and compared to the comprehensively studied $La_{0.8}Sr_{0.2}FeO_3$ (LSF-20) composition. With the exception of Ca, all variants showed either increased reactivity with YSZ (compared to the base LSF-20), or a lack of phase purity after calcination at 1200–1300 °C.

Keywords: Reactivity; Lanthanide ferrite; SOFC cathodes

1. Introduction

In recent years there has been intensive study into the use of mixed conducting ABO_3 perovskites for use as solid oxide fuel cell (SOFC) cathodes. A promising candidate is $La_{0.8}Sr_{0.2}FeO_3$ (LSF-20), which when used in conjunction with an anode-supported yttria-stabilized zirconia (YSZ) electrolyte assembly, achieves power densities of 0.8–0.95 W/cm^2 at 750 °C and 0.7 V [1]. However, this performance relies on the incorporation of a doped ceria interlayer, $Ce_{0.8}Sm_{0.2}O_{1.9}$ (SDC-20), between the YSZ electrolyte and LSF cathode. The ceria acts as a protective barrier preventing LSF-YSZ reaction during the cathode sintering step (typically 1100–1200 °C). The interaction involves the diffusion of Zr^{4+} cations into the perovskite (and an accompanying increase in unit cell volume readily detected by X-ray diffraction) where they occupy B-site positions, and result in decreased electrical (and possibly ionic) conductivity of the cathode [2]. As expected the Zr diffusion exhibits thermal dependence, and is typically observed at temperatures ≥950 °C. Fig. 1 indicates the decreased performance of an LSF-20 cathode sintered at 1150 °C directly onto YSZ (∼650 mW/cm^2 0.7 V/750 °C) compared to that utilizing the protective ceria layer (∼950 mW/cm^2 0.7 V/750 °C). Whilst the aforementioned LSF-SDC configuration indicates reasonable performance, from a processing (cost) standpoint it is desirable to negate the need for the protective ceria interlayer. In addition, there are concerns with the reactivity of YSZ and SDC. To achieve adequate adherence of the SDC interlayer, sintering temperatures of ∼1200 °C are required, and at this temperature ceria and YSZ react to form a solid solution with poor oxygen ion conductivity [3]. This study considers the possibility of reducing the cathode-YSZ interaction with A-site primary and dopant cation modifications, in particular substitution of La with Pr, Nd, Sm and Ln (mixed lanthanide precursor), and Sr with Ca and Ba.

2. Experimental

All ferrite cathode powders used in this study were produced by glycine-nitrate combustion synthesis [4], and then calcined at 1200–1300 °C for 2 h. The chemical composition of the mixed lanthanide (Ln) nitrate precursor is detailed in Table 1. Powders were tested for phase purity via X-ray diffraction (XRD) using a Philips Wide-Range Vertical Goniometer and a Philips XRG3100 X-ray Generator over a range of 20–65° 2θ and a step size of 0.02° with a hold time of 1–2 s. These powders were added to a commercially-supplied yttrium-stabilized zirconia (8-YSZ) in a 50/50 vol.% ratio, and thoroughly mixed for 24 h via ball milling. The resulting mixtures were then pressed into bars uniaxially to 1.72 MPa and then isostatically to 3.45 MPa to a final size of approximately 45 mm × 16 mm × 3 mm and final weight of approximately 10 g. These in turn were reacted from 1000 to 1200 °C for 2 h. Reacted samples were

* Corresponding author. Tel.: +1-509-943-6264; fax: +1-509-375-2186.
E-mail address: steven.simner@pnl.gov (S.P. Simner).

0378-7753/$ – see front matter © 2003 Elsevier B.V. All rights reserved.
doi:10.1016/j.jpowsour.2003.11.039

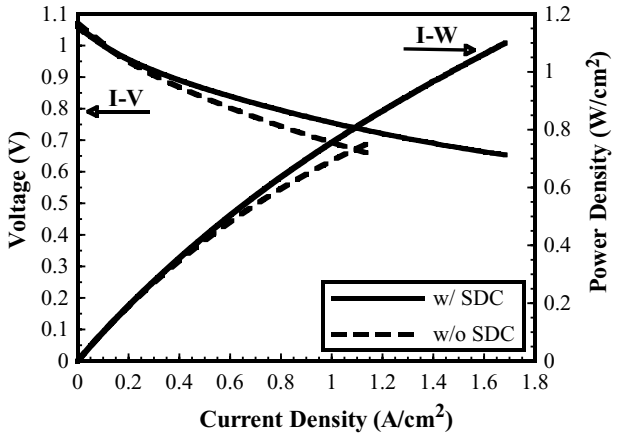

Fig. 1. Cell performance data comparing LSF-20 cathodes on anode-supported YSZ substrates with and without a ceria interlayer between the cathode and electrolyte.

Table 1
Chemical analysis of mixed lanthanide precursor

Oxide	Concentration (wt.%)
La_2O_3	70.50
Nd_2O_3	14.27
CeO_2	8.50
Pr_2O_3	3.53
Eu_2O_3	1.66
Sm_2O_3	0.66
Gd_2O_3, Y_2O_3, Al_2O_3, SiO_2, SrO and CaO	Balance

again analyzed by XRD for phase impurities, and subsequently mixed with 20 wt.% NIST Si standard (SRM 640c) and re-analyzed by XRD to enable accurate unit cell volume determination. Sintering shrinkage analysis of selected cathode compositions (calcined at 800 °C) was carried out in a Unitherm Model 1161 vertical pushrod dilatometer with a 40 g load from room temperature to 1200°C at a heating rate of 3 °C/min.

3. Results and discussion

Of the various cation modifications attempted compounds incorporating neodymium, barium and the mixed lanthanide did not demonstrate phase purity after calcination at 1200 °C (Table 2). Additional calcination at 1300 °C was likewise unsuccessful, and hence these compounds were not examined further. Moreover, those cathode compositions that indicated significant reactivity with YSZ at 1200 °C were not subjected to additional analysis, since our experience with SOFC materials has indicated that the reaction of adjacent cell materials is rarely (if ever) a beneficial occurrence. The mixed lanthanide ferrite ($Ln_{0.8}Sr_{0.2}FeO_3$) indicated a variety of reaction phases including >10 wt.% $La_2Zr_2O_7$ and/or CeO_2 (the major XRD peak positions are very closely alligned for these 2 compositions), in addition to Fe_3O_4 and $Sr_2Fe_2O_5$. $Sm_{0.8}Sr_{0.2}FeO_3$ also indicated reactivity with YSZ at 1200 °C resulting in the formation of >10 wt.% $Sm_{0.8}Zr_{0.2}O_{1.6}$.

Table 2
XRD phase data for calcined and reacted cathode compositions

Composition	Calcination at 1200 °C (wt.% of secondary phases)	Reaction with 8-YSZ at 1200 °C (wt.% of secondary phases)
$La_{0.8}Sr_{0.2}FeO_3$	None	T $SrFe_{12}O_{19}$ (??)
$Pr_{0.8}Sr_{0.2}FeO_3$	None	T unidentified
$Nd_{0.8}Sr_{0.2}FeO_3$	>10 wt.% $Sr_3Fe_2O_{6.64}$ >5 wt.% Nd_2O_3	NA
$Sm_{0.8}Sr_{0.2}FeO_3$	None	>10 wt.% $Sm_{0.8}Zr_{0.2}O_{1.6}$ M unidentified
$Ln_{0.8}Sr_{0.2}FeO_3$	T CeO_2 (??)	>10 wt.% La_2Zr_2O7 (and/or CeO_2) >5 wt.% Fe_3O_4 M $Sr_2Fe_2O_5$ T Y_2O_3 T $La_2SrFe_2O_7$ T $La_{0.5}Sr_{0.5}FeO_3$
$La_{0.8}Ba_{0.2}FeO_3$	>10 wt.% La_2O_3 T BaO	NA
$La_{0.8}Ca_{0.2}FeO_3$	None	T Fe_2O_3 T Y_2O_3 (??)

T: trace amount <2 wt.%; M: minor amount 2–5 wt.%; NA: not analyzed; ??: only the 100% peak discernible and barely above background.

The findings for the reactivity of the remaining cathode compositions (in terms of secondary phase formation and/or X-ray peak shifts indicating Zr incorporation into the perovskite) are detailed below. These materials were also subjected to additional reaction temperatures of 1000° and 1100 °C to establish potential patterns in their reactivities with YSZ.

3.1. $La_{0.8}Sr_{0.2}FeO_3$ (LSF-20)

The reactivity of this composition with 8-YSZ has also been discussed in greater detail in a previous publication [2]. Fig. 2 (Table 3) indicate XRD pattern (and unit cell volume) data for LSF-20/8-YSZ compositions reacted from 1000 to 1200 °C and compared to a non-reacted sample. As observed in the previous study [2], most noticeable is the shift of the LSF peak to the left indicative of a volume expansion, caused by the dissolution of larger Zr cations (see Table 4 [5]) onto the perovskite B-site. The shift is marginal after reaction at 1000 °C, whereas for temperatures ≥1100 °C the unit cell expansion is fairly significant (between 2 and 3 vol.%). It should also be noted that the unit cell volume of the YSZ appeared unchanged between the non-reacted and reacted samples. This is despite the fact that Zr cations are leaving the fluorite structure, and presumably causing Y-enrichment. However, fairly significant changes in Y concentration do not manifest as readily detectable shifts in the XRD pattern; e.g. YSZ-9 100% peak position = 30.068°, unit cell

Table 3
Unit cell volume (Å^3) data of cathode and YSZ structures after reaction from 1000 to 1200 °C

Cathode mixed with 8-YSZ	RT °C		1000 °C		1100 °C		1200 °C	
	ABO_3	YSZ	ABO_3	YSZ	ABO_3	YSZ	ABO_3	YSZ
$La_{0.8}Sr_{0.2}FeO_3$	239.82	67.84	240.35	67.82	245.4	67.77	246.63	67.74
$Pr_{0.8}Sr_{0.2}FeO_3$	237.92	67.79	237.60	67.88	240.23	69.59	241.57	69.47
$La_{0.8}Ca_{0.2}FeO_3$	237.60	67.79	240.04	67.63	241.14	67.78	241.60	67.79

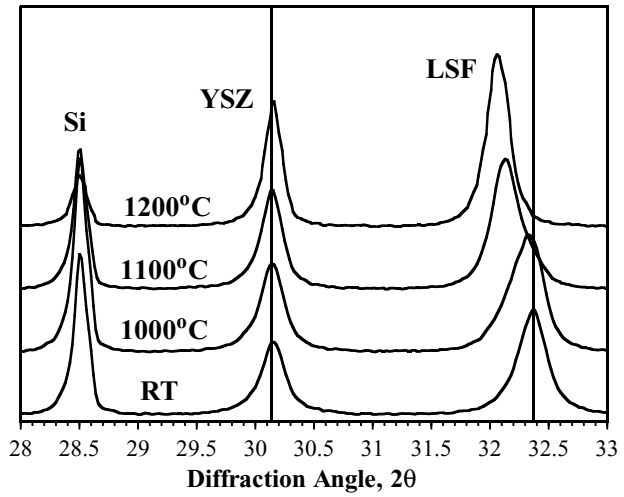

Fig. 2. X-ray diffraction data of LSF-20/8-YSZ mixtures reacted from 1000 to 1200 °C, and compared to an un-reacted sample.

volume = 68.03 Å^3 [6], YSZ-5 100% peak position = 30.134°, unit cell volume = 67.60 Å^3 [6]—a 2θ difference of only 0.066°. Hence, such small shifts in the YSZ peaks are difficult to resolve with assured accuracy.

Additionally, Table 2 suggests the existence of trace $SrFe_{12}O_{19}$, but its presence can only be considered tentative since the 100% peak was barely discernible above background. Such a phase was not observed in the previous investigation even after reaction at 1400 °C [2], and the absence of Fe-rich oxides as second phases was considered plausible (despite considerable dissolution of Zr onto the LSF B-site) given the findings of a recent study by Carter et al. [7], in which LSF compounds with 20% A-site deficiencies remained phase pure.

Table 4
Ionic radii for relevant perovskite and fluorite cations [5]

Cation	Ionic radii (Å) for specific coordination numbers		
	12	8	6
Zr^{4+}	–	0.84	0.72
Y^{3+}	–	1.019	0.90
La^{3+}	1.36	1.16	1.032
Pr^{3+}	–	1.126	0.99
Pr^{4+}	–	0.96	0.85
Sr^{2+}	1.44	1.26	1.18
Ca^{2+}	1.34	1.12	1.00
Fe^{2+}	–	0.92	0.61 LS, 0.78 HS
Fe^{3+}	–	0.78	0.55 LS, 0.645 HS
Fe^{4+}	–	–	0.585

Coordination numbers: Perovskite ABO_3 → 12:6:6; Fluorite AO_2 → 8:4.

3.2. $La_{0.8}Ca_{0.2}FeO_3$ (LCF-20)

Unlike the LSF-20 composition LCF-20 indicates a significant peak shift at 1000 °C, but little subsequent shift at the higher reaction temperatures (Fig. 3). After reaction at 1200 °C the unit cell expansion of LCF (compared to the un-reacted material) is ~1.7% compared to ~2.8% for the LSF sample. This may be a consequence of a lower limit of Zr dissolution into the LCF compound due to its smaller unit cell volume (Table 3), which results from the smaller Ca cation radius compared to Sr (Table 4 [5]). Unlike the LSF-20 sample, LCF also indicates precipitation of trace Fe_2O_3 above 1000 °C. Presumably the LCF is not capable of such large A-site deficiency, and Zr dissolution results in Fe-oxide precipitation.

To analyze the comparative Zr contents achievable in LCF and LSF the following compounds were synthesized: $La_{0.8}Sr_{0.2}Fe_{1.0}Zr_{0.1}O_3$ (LSFZr-82101) and $La_{0.8}Ca_{0.2}Fe_{1.0}Zr_{0.1}O_3$ (LCFZr-82101) (A/B cation ratio =~ 0.91). Fig. 4 compares XRD traces for both compounds after calcinations at 1200 °C. The unit cell volume of each perovskite is labeled on the respective XRD trace, and when compared to the un-reacted LSF or LCF powders (Table 3), both of the Zr-doped compositions indicate

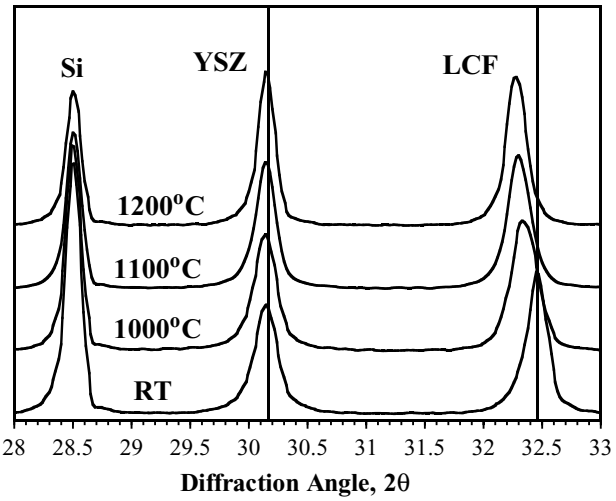

Fig. 3. X-ray diffraction data of LCF-20/8-YSZ mixtures reacted from 1000 to 1200 °C, and compared to an un-reacted sample.

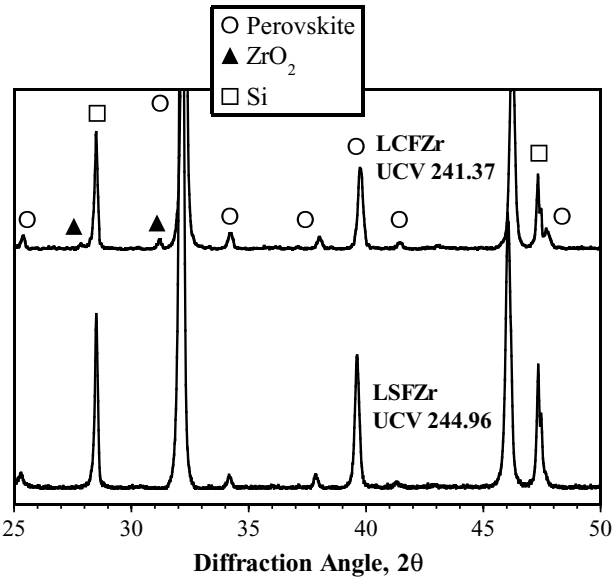

Fig. 4. X-ray diffraction data of LSFZr-82101 and LCFZr-82101 compositions calcined at 1200 °C for 2 h.

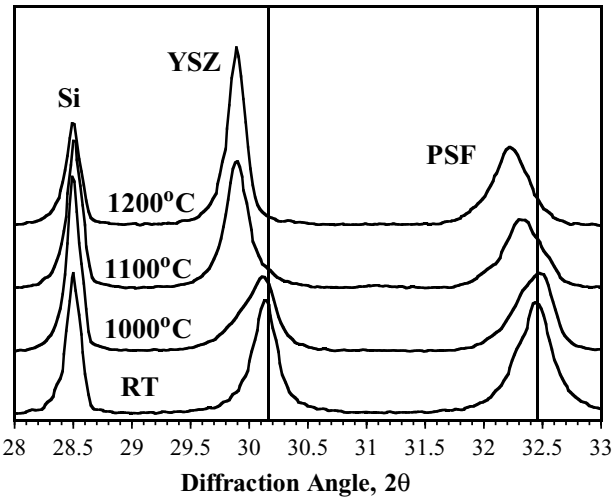

Fig. 5. X-ray diffraction data of PSF-20/8-YSZ mixtures reacted from 1000 to 1200 °C, and compared to an un-reacted sample.

expansion indicative of Zr cation incorporation. More interestingly, however, is the fact that the LSFZr compound appears phase pure (though again there is marginal indication that $SrFe_{12}O_{19}$ may be precipitated) while the LCFZr sample exhibits ZrO_2 as a second phase. This indicates that Zr is more easily accommodated within the LSF structure than the LCF perovskite. As forementioned this is presumably due to the lower initial cell volume of the LCF due to the smaller Ca^{2+} ionic radius (Table 4). This finding suggests that it may be possible to manipulate the perovskite structure to achieve even lower unit cell volumes with lower Zr dissolution limits. It should be noted that whilst the presence of ZrO_2 was verified by representative peaks across the entire scan range (20–65° 2θ), the peak intensity at ~31° 2θ was somewhat higher than that indicated by the PDF file (72–0597). This suggests the possible presence of at least one additional impurity phase, and subsequent combination of peaks at 31° 2θ. Unfortunately, additional phases could not be positively identified.

3.3. $Pr_{0.8}Sr_{0.2}FeO_3$ (PSF-20)

PSF-20/8-YSZ reactivity is interesting in that the both the PSF and YSZ peaks shift to the left (Fig. 5). It is conceivable that Pr^{3+} replaces Y^{3+}, or Pr^{4+} replaces Zr^{4+}—according to Table 4 both would induce a unit cell expansion of the YSZ. However, if large proportions of Pr cations are dissolving into the fluorite structure, the perovskite would be left highly A-site deficient—as forementioned the structure may be able to accommodate the depletion of A-site cations. No Fe-rich oxides are detected by XRD. It is also possible that both Y^{3+} and Zr^{4+} migrate to the perovskite A- and B-sites, respectively to maintain stoichiometry. Essentially the reactivity of PSF and YSZ is somewhat more complicated than the other cathode-YSZ combinations in this study, and may warrant further investigation. PSF-20 also indicates trace $SrZrO_3$ at 1100 °C which subsequently disappears after reaction at 1200 °C.

4. Sintering srinkage

The reactivity of the cathode samples with YSZ may be less significant if the sample can be sintered below the reaction onset temperature. Fig. 6 indicates sintering shrinkage data for LSF-20, LCF-20 and PSF-20. PSF-20 has low sintering activity and would require a temperature of >1200 °C to achieve adequate cathode adherence, which would initiate considerable reactivity with the YSZ electrolyte. It has already been established that at the typical sintering temperature for LSF-20 of 1150–1200 °C, LSF-YSZ interaction readily occurs. On the other hand, LCF-20 indicates significantly enhanced sintering activity, and may be sinterable on

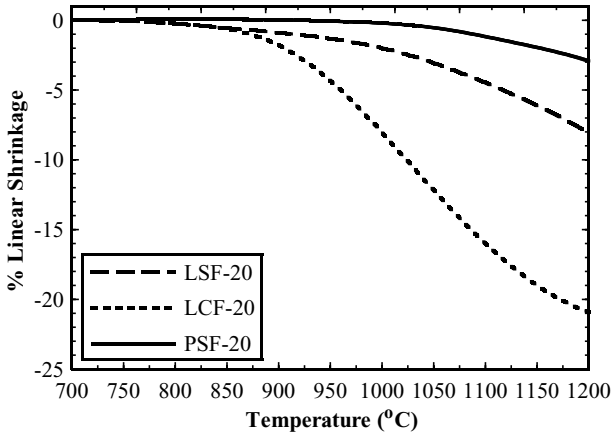

Fig. 6. Sintering shrinkage data for LSF-20, LCF-20 and PSF-20.

YSZ from 1000 to 1100 °C. The LCF-20 is also attractive from the standpoint that the degree of Zr incorporation is less than that observed for LSF, and above a reaction temperature of 1000 °C there appears to be little increase in the unit cell volume and hence Zr dissolution.

5. Conclusion

Despite various modifications in primary and dopant A-site cations, lanthanide ferrite compounds still exhibit reactivity with 8-YSZ. The reactivity either results in secondary phase formation or incorporation of Zr onto the perovskite B-site. From this study, the most promising candidate for direct application to YSZ is probably $La_{0.8}Ca_{0.2}FeO_3$ since it indicates decreased dissolution of Zr into the perovskite at 1200 °C, and the ability to be sintered from 1000 to 1100 °C, potentially avoiding any major interaction with the YSZ.

Acknowledgements

Supported by the Solid-State Energy Conversion Alliance (SECA) Core Technology Program by the US Department of Energy's National Energy Technology Laboratory (NETL). PNNL is operated by Battelle Memorial Institute for the US Department of Energy under Contract DE-AC06-76RL.

References

[1] S.P. Simner, J.F. Bonnett, N.L. Canfield, K.D. Meinhardt, V.L. Sprenkle, J.W. Stevenson, Optimized lanthanum ferrite-based cathodes for anode-supported SOFCs, Electrochem. Solid State Lett. 5 (7) (2002) A173–A175.
[2] S.P. Simner, J.P. Shelton, M.D. Anderson, J.W. Stevenson, Interaction between La(Sr)FeO_3 SOFC cathode and YSZ electrolyte, Solid State Ionics 161 (2003) 11–18.
[3] A. Tsoga, A. Gupta, A. Naoumidis, P. Nikolopoulos, Gadolinia-doped ceria and yttria stabilzed zirconia interfaces: regarding their application for SOFC technology, Acta Mater. 48 (2000) 4709–4714.
[4] L.A. Chick, L.R. Pederson, G.D. Maupin, J.L. Bates, L.E. Thomas, G.J. Exarhos, Synthesis of oxide ceramic powders by the glycine-nitrate process, Mater. Lett. 10 (1–2) (1990) 6–11.
[5] R.D. Shannon, Revised effective ionic radii and systematic studies of interatomic distances in halides and chalcogenides, Acta Cryst. A32 (1976) 751–767.
[6] M. Yashima, S. Sasaki, S. Kakihana, M. Yamaguchi, H. Arashi, M. Yoshimura, Acta Cryst. Sec. B Struct. Sci. 50 (1994) 663.
[7] J.D. Carter, J.M. Ralph, J.-M. Bae, T.A. Cruse, C.C. Rossignol, M. Krumpelt, R. Kumar, Improved materials and cell design for mechanically robust solid oxide fuel cells, in: Proceedings of the 2002 Fuel Cell Seminar, Palm Springs, CA, 2002, p. 874.